

Helical Magnetic Fields Associated with the Relativistic Jets of Four BL Lac Objects

Denise C. Gabuzda, Éamonn Murray & Patrick Cronin¹

¹*Department of Physics, University College Cork, Cork, Ireland*

2 February 2008

ABSTRACT

Evidence has been mounting that many of the transverse jet \mathbf{B} fields observed in BL Lac objects on parsec scales represent the dominant vvoidal component of the intrinsic jet \mathbf{B} fields. Such fields could come about, for example, as a result of the “winding up” of an initial “seed” field with a significant longitudinal component by the rotation of the central accreting object. If this is the case, this should give rise to gradients in the rotation measure (RM) across the jets, due to the systematic change in the line-of-sight component of the jet \mathbf{B} field. We present evidence for transverse RM gradients in four BL Lac objects, strengthening arguments that the jets of these objects do indeed have toroidal or helical \mathbf{B} fields. This underlines the view of the jets as fundamentally electromagnetic structures, and suggests that they may well carry non-zero currents. It also provides a natural means to collimate the jets.

Key words: polarization – radio sources: galaxies

1 INTRODUCTION

BL Lac objects are highly variable, appreciably polarized Active Galactic Nuclei (AGN) that are observationally similar to radio-loud quasars in many respects, but display systematically weaker optical line emission, whose origin is not clear. Very Long Baseline Interferometry (VLBI) polarization observations of radio-loud BL Lac objects have shown a tendency for the polarization \mathbf{E} vectors in the parsec-scale jets to be aligned with the local jet direction; since the jet emission is optically thin, this implies that the corresponding magnetic \mathbf{B} field is transverse to the jet (Gabuzda, Pushkarev, & Cawthorne 2000 & references therein). This has usually been interpreted as evidence for relativistic shocks that enhance the \mathbf{B} -field component in the plane of compression, perpendicular to the direction of propagation of the shock (Laing 1980; Hughes, Aller, & Aller 1989).

However, as the quality of VLBI polarization images has improved and images have become available for a larger number of objects at a larger number of wavelengths, evidence has been building that many of the observed jet \mathbf{B} fields actually correspond to the “intrinsic” \mathbf{B} fields of the VLBI jets themselves. For example, in a number of BL Lac objects, the observed polarization vectors remain aligned with the jet over extensive sections of the jet, even in the presence of appreciable bending (0954+658: Gabuzda & Cawthorne 1996; 1803+784: Gabuzda 1999; 0823+033 and 1749+701: Gabuzda & Pushkarev 2002). A interpretation in the framework of shock models requires the presence of a

series of relativistic shocks along the jet, each of which enhances the local transverse \mathbf{B} field. Although theoretically possible, this picture seems contrived. An alternative is that the observed transverse \mathbf{B} fields in these sources are associated with the dominant toroidal component of the intrinsic jet \mathbf{B} fields, in which case maintenance of the transverse field orientation as the jets curve would be natural.

In addition, we might expect energetic shocks to be relatively compact features, while some individual VLBI features that display transverse \mathbf{B} -field structures are far from compact (e.g. 1219+285: Gabuzda et al. 1994, 1803+784: Gabuzda & Chernetskii 2003). A number of jets with alternating aligned and orthogonal polarization vectors (orthogonal and aligned \mathbf{B} -field structures) have also recently been discovered (e.g. OJ287: Gabuzda & Gómez 2001; 1418+546: Gabuzda 2003). In the standard picture, these would correspond to fields ordered by local phenomena at various places in the jet; however, a view in which these alternating \mathbf{B} fields represent oscillations or instabilities of a global jet \mathbf{B} field might be simpler.

Further, if a jet has a helical \mathbf{B} field, the observed \mathbf{B} -field structure will depend on both the degree of dominance of the toroidal component and the viewing angle. The viewing angle will play a role both geometrically and in terms of relativistic aberration effects. For example, if the inferred observed \mathbf{B} field is everywhere transverse, with little or no sign of a longitudinal component near the edges, this would require that we are viewing the jet nearly “side-on” (i.e., at 90° to its axis) in its rest frame; if such a jet

is viewed at an angle that differs from 90° to its axis in its rest frame, we should see a central region of transverse **B** field with regions of longitudinal field appearing near the edges of the jet. In fact, a number of compact AGN displaying just such “spine+sheath” **B**-field structures have been observed. The first example was 1055+018 (Attridge, Roberts & Wardle 1999), and such structures have since been observed in 0820+225 (Gabuzda, Pushkarev & Garnich 2001), 0745+241 (Pushkarev & Gabuzda 2002), and 1652+398 (Gabuzda 2003c). This has sometimes been interpreted in the shock paradigm as representing jets with series of shocks that are also interacting with a surrounding medium (Attridge, Roberts & Wardle 1999). However, as is indicated above, the hypothesis that some AGN jets have helical **B** fields can also provide a simple explanation for these “spine+sheath” structures.

Jet fields with an observed dominant toroidal component could come about very naturally as a result of the “winding up” of an initial “seed” field with a significant longitudinal component by the rotation of the central accreting object (e.g. Nakamura, Uchida, & Hirose 2001; Lovelace et al. 2002; Hujeirat et al. 2003; Lynden-Bell 2003; Tsinganos & Bogovalov 2002). Another intriguing possibility is that the observed toroidal field components develop in association with currents flowing in the jet (Pariev et al. 2003; Lyutikov 2003). Indeed, if there is a dominant toroidal **B**-field component, basic physics tells us that in some sense there *must* be currents flowing in the region enclosed by the field.

It is therefore of interest to identify robust observational tests that can distinguish between transverse **B** fields due to a toroidal field component and due to shock compression. One such diagnostic is provided by Faraday rotation – rotation of the observed plane of linear polarization due to propagation of the polarized radiation through a magnetized plasma. The rotation of the polarization angle χ is determined by the observing wavelength λ , and the density of free electrons $N(s)$ and the line-of-sight component of the **B** field in the plasma (e.g. Burn 1966):

$$\begin{aligned}\chi &= \chi_0 + \frac{e^3 \lambda^2}{8\pi m_e^2 \epsilon_0 c} \int N(s) \vec{B}(s) \cdot ds \\ \chi &= \chi_0 + \text{RM} \lambda^2\end{aligned}$$

where χ_0 is the intrinsic polarization angle, e is the electron charge, m_e is the electron mass, and the integral is taken over the line of sight from the source to the observer. Faraday rotation can be identified via the characteristic quadratic dependence of the rotation of χ on the observing wavelength; the coefficient of λ^2 is called the rotation measure (RM). In the case of a toroidal or helical jet **B** field, we should observe a gradient in the observed Faraday rotation *across* the jet, due to the systematic change in the line-of-sight component of the **B** field across the jet (see, e.g., Blandford 1993). Asada et al. (2002) claim to have detected such a gradient across the VLBI jet of 3C273, and interpreted this as evidence that this jet has a helical **B** field.

In light of this result, we conducted a search for transverse RM gradients among sources from a complete sample of northern BL Lac objects (Kühr & Schmidt 1990) for which we had simultaneous VLBI polarization data at 2, 4, and 6 cm obtained on the Very Long Baseline Array (VLBA). We present here results for four of these sources in which we

Table 1. Q AND U NOISE LEVELS AND χ UNCERTAINTIES

2 cm		4 cm		6 cm		Max $\Delta\chi$ (deg)
Q (mJy/ beam)	U (mJy/ beam)	Q (mJy/ beam)	U (mJy/ beam)	Q (mJy/ beam)	U (mJy/ beam)	
			0745+241			
0.40	0.48	0.23	0.26	0.17	0.23	6
			0820+225			
0.21	0.21	0.20	0.13	0.18	0.17	5
			1652+398			
0.45	0.47	0.19	0.18	0.22	0.23	8
			3C371			
0.56	0.62	0.25	0.32	0.29	0.31	7

have detected clear RM gradients transverse to the VLBI jets. It is natural to interpret the observed RM gradients as revealing a toroidal or helical **B** field associated with these VLBI jets, particularly given the other evidence that points in this direction.

2 OBSERVATIONS AND REDUCTION

The polarization observations considered here were carried out on February 9, 1997 at 6, 4 & 2 cm using the NRAO Very Long Baseline Array, as part of an ongoing study of the complete sample of northern BL Lac objects defined by Kühr & Schmidt (1990). In all cases, the sources were observed in a “snapshot” mode, with roughly 8–10 scans of each object spread out over the time the source was visible with most or all of the VLBA antennas; the resulting coverage of the u – v plane was quite uniform. The data reduction and imaging were done in the AIPS package using standard techniques.

The instrumental polarizations (“D-terms”) were derived from observations of the unpolarized source 3C84 using the AIPS task LPCAL. The calibration of the absolute electric vector position angles (EVPAs) was determined using integrated polarization measurements obtained during a VLA session of about two hours duration on February 12, 1997. The primary EVPA calibrator used to calibrate the VLA polarization position angles was 3C286 (assuming $2\chi = 66^\circ$, in the standard fashion). The VLBI EVPAs were calibrated by requiring that the EVPA for the total VLBI polarization of a compact source coincide with the EVPA for the VLA core. The source used for this purpose were 1823+568, for which more than 90% of the VLA core polarization is present on VLBI scales (e.g. Gabuzda et al. 1992). The near simultaneity of the VLA and VLBA observations minimizes the possibility of variations in the source polarization between the dates of the VLA and VLBA observations. We estimate that these EVPA calibrations are accurate to within about 3° .

Note that any errors in the EVPA calibration affect all polarization angles in all regions of all the sources in the same way, and so could not lead to the presence of spurious Faraday-rotation gradients in the source structure.

We made maps of the distribution of the 2, 4 and 6-cm total intensity I and Stokes parameters Q and U with matched resolutions corresponding to the 6-cm beam; in the case of 0820+225, the beam used for the matched-resolution maps was 1.5 times the size of the 6-cm beam. The Q and

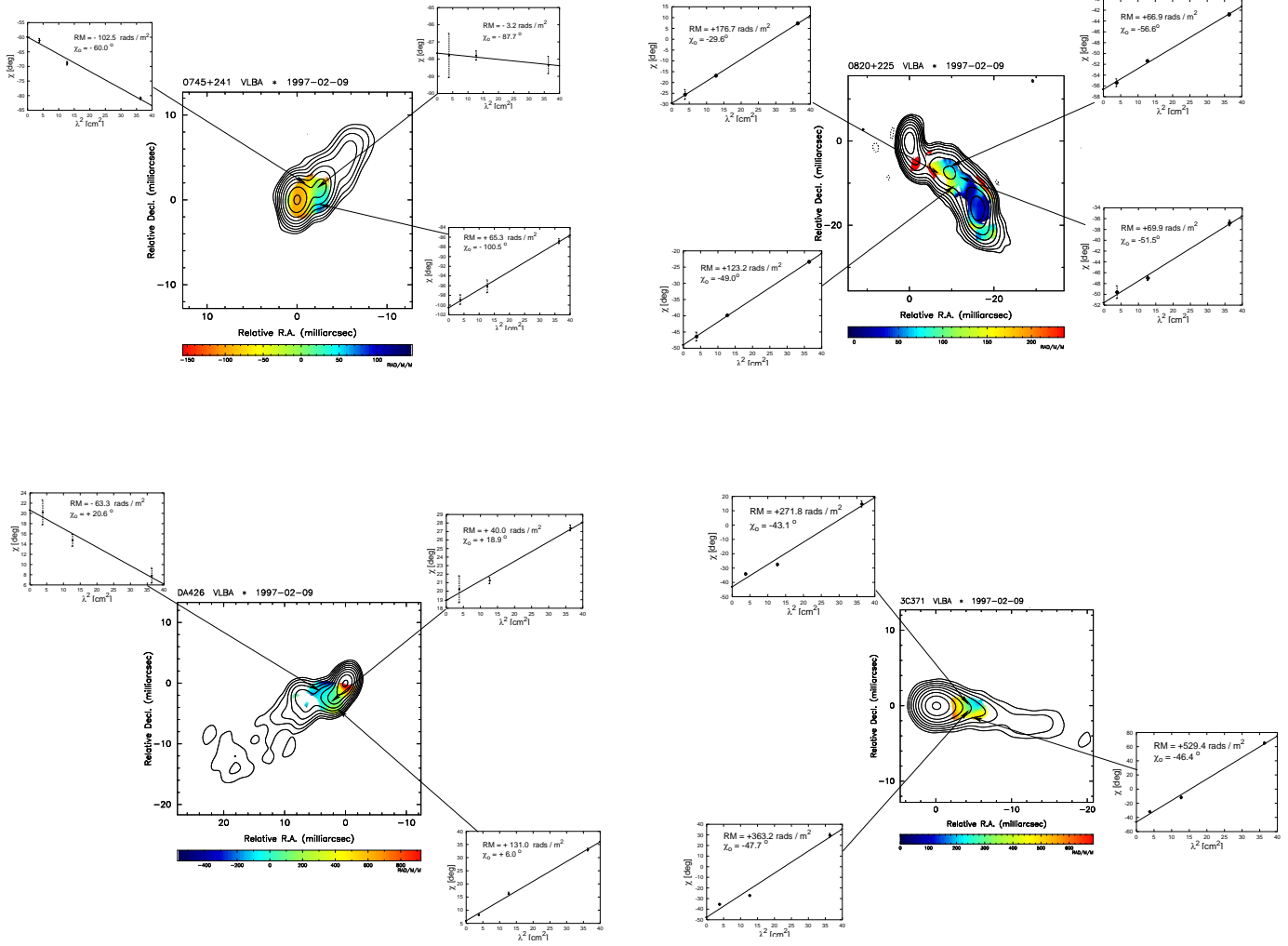


Figure 1. 6 cm VLBI I maps of 0745+241 (top left), 0820+225 (top right), 1652+398 (bottom left) and 3C371 (bottom right), with the parsec-scale RM distributions superimposed. The accompanying graphs show plots of χ vs. λ^2 for several locations across the VLBI jets. The χ errors shown are 1σ . The convolving beams used for both the total-intensity and RM distributions are 2.79×1.72 mas in $PA = -4^\circ$ for 0745+241, 4.38×2.58 mas in $PA = -6^\circ$ for 0820+225, 2.55×1.89 mas in $PA = -24^\circ$ for 1652+398 and 2.47×2.9 mas in $PA = -83^\circ$ for 3C371.

U maps were then used to construct the distributions of the polarized flux ($p = \sqrt{Q^2 + U^2}$) and polarization angle ($\chi = \frac{1}{2} \arctan \frac{U}{Q}$), as well as accompanying “noise maps,” using the AIPS task COMB. The formal uncertainties written in the output χ noise maps were calculated in COMB using the rms noise levels on the input Q and U maps, summarized in the Table.

Before making the final RM maps using the AIPS task RM, we first removed the contribution of the known integrated (predominantly Galactic, i.e., foreground; Pushkarev 2001) Faraday rotation at each wavelength, so that any remaining non-zero rotation measure should be due to thermal plasma in the vicinity of the AGN. The task RM has the option of blanking output values in pixels for which the χ errors at any of the three wavelengths used are larger than a specified value. The maximum χ uncertainties for a single

pixel applied to construct the rotation-measure maps shown in Fig. 1 are also indicated in the Table.

For the purposes of determining the χ values for individual regions in the VLBI jet, we found the mean within a 3×3 pixel (0.3×0.3 mas) area (i.e., nine elements) at the corresponding location in the map; the errors in these polarization angles were taken to be the rms deviation from this mean value.

3 RESULTS

Fig. 1 shows the 6-cm VLBI I images of four objects displaying transverse RM gradients with color images of their parsec-scale RM distributions superposed. The convolving beams used in each case are indicated in the figure caption. The RM gradients across the VLBI jets are visible by eye.

The accompanying plots show the observed polarization position angles, χ , as a function of the observing wavelength squared, λ^2 , for individual locations in the VLBI jets. The χ errors shown are 1σ . In all cases, the observed χ values are in good agreement with the λ^2 law expected for Faraday rotation.

Fig. 2 shows plots of the observed RMs with their errors as a function of approximate transverse distance from the central spine of the VLBI jets of each of the four objects; the point from which the distances were measured and the position angle along which they were measured are indicated in the figure caption. The errors in the RMs were estimated in two ways: (i) in the same way as for the χ values, by calculating the mean RM within the corresponding 3×3 pixel (0.3×0.3 mas) area (i.e., nine elements) in the map and assigning the rms deviation about this mean as the RM error, and (ii) from the linear fit to χ vs. λ^2 . In most cases, these two methods gave comparable errors, but if there was a significant difference in the two errors, we adopted the larger of the two as the error in the RM, in order to help ensure that the errors were not severely underestimated. Fig. 2 confirms that the transverse RM gradients are highly significant. The differences between the two RM values on either side of the central spine of the jets are 8.5σ for 0745+241, 18.6σ and 6.7σ for 0820+225 (for transverse cuts roughly 10 mas and 15 mas from the core, respectively), 9.4σ for 1652+398 and 8.2σ for 3C371. This leaves no doubt of the reality of the observed transverse RM gradients.

4 DISCUSSION

In order to obtain the RM distributions shown, it was necessary to convolve the 2-cm Q and U images with a beam that was roughly three times the beam corresponding to the intrinsic resolution of the 2-cm data. This might give rise to concerns that a blending of 2-cm and 4-cm polarized components located within the 6-cm beam could lead to the appearance of false structure in the resulting RM maps. In none of the four sources considered here was there transverse structure in the jet polarization in the regions shown in the RM maps that was evident at the shorter wavelengths, but not at 6 cm. Two additional facts convince us that the observed RM gradients are not spurious structures resulting from the need to use a single convolving beam when constructing the images at all three wavelengths: (i) the gradients are systematic and monotonic, and (ii) in all cases, the observed χ values display a clear λ^2 dependence, demonstrating that we are seeing the manifestation of Faraday rotation.

An independent 2+4+6 cm VLBA RM map for 1652+398 (= Mrk501) for epoch April 1998 analyzed by Croke et al. (2004) shows a transverse RM gradient with the same sense and covering roughly the same range of rotation measures as the RM map of this source shown in Fig. 1. A preliminary analysis of 6, 13, and 18-cm VLBA polarization data for this source for May 1998 also displays a transverse RM gradient in the same sense (Croke et al., in preparation). These independent RM distributions serve to confirm the reality of the gradients we have detected in this source.

The transverse rotation-measure gradients observed in

0745+241 and 1652+398 (left panels in Fig. 1) are positive on one side of the jet spine and negative on the other. This behaviour is expected if we are viewing the jet nearly orthogonal to its axis *in the source frame*. If the Lorentz factor for the jet's motion is γ , photons emitted at 90° to the jet axis in the source frame will be observed in the observer's frame to propagate at an angle $\theta = 1/\gamma$ to the jet axis. Since we believe that compact radio-loud AGN such as BL Lac objects represent precisely those sources whose jets are viewed at small angles to the line of sight, it is quite natural to observe this behaviour in the rotation-measure gradients. If the jet is viewed at an angle somewhat different than 90° to the jet axis in the source frame, this will lead to an offset in the observed RM gradients, so that the observed RM will not be symmetrical about a rotation measure of zero; this can qualitatively explain the RM gradients observed for 0820+225 and 3C371 (right panels in Fig. 1).

Because relativistic boosting of the jet emission changes the relative strength of the \mathbf{B} -field components along and orthogonal to the line of sight, the toroidal \mathbf{B} -field component will become dominant in the observer's frame, even if the toroidal and poloidal \mathbf{B} -field components in the source frame are comparable (e.g., Blandford & Königl 1979; this is discussed in more detail by Lyutikov, Pariev & Gabuzda, in preparation). This could provide a natural explanation for why Faraday-rotation gradients transverse to the jet axis appear to be fairly common among the objects we have studied.

The presence of a helical \mathbf{B} field carried outward with the relativistic outflows provides a natural mechanism for the collimation of these outflows, which in some cases remain extremely well collimated out to kiloparsec scales. Although it is difficult to prove conclusively, the presence of toroidal or helical \mathbf{B} fields genetically related to the relativistic jets suggests that a significant fraction of their energy may be carried by the ordered component of the magnetic field, rather than by the hydrodynamical energy of the flow.

Another intriguing possibility is that a connection will emerge between the evidence we have found for helical \mathbf{B} fields associated with these four BL Lac objects and the recent detection of circular polarization in the core regions of a number of AGN (Homan, Attridge & Wardle 2001, Gabuzda & Vitrishchak 2004). It is possible that both the helical fields and the circular polarization are associated with the rotation of the central black hole and accretion disk; in this case, there should be a direct relationship between the transverse RM gradients (which reflect the direction of the rotation) and the sign of the circular polarization. There are two sources for which both transverse RM gradients and parsec-scale circular polarization have been detected: 3C273 and 1807+398 (= 3C371). In the case of 3C273, the jet propagates to the southwest, and the RM is more positive along the northwestern edge of the jet, implying that the rotation of the accretion disk is *clockwise* as viewed by the observer (Asada et al. 2002); the VLBI core circular polarization measured by Homan & Wardle (1999) was *negative*. In the case of 3C371, the VLBI jet propagates toward the west and the RM is more positive along the southern edge of the jet, implying that the rotation of the accretion disk is *counterclockwise* as viewed by the observer; the VLBI core circular polarization measured by Gabuzda & Vitrishchak (2004) was *positive*. Thus, these two cases are consistent with both the transverse RM gradients and the parsec-scale circular polarization.

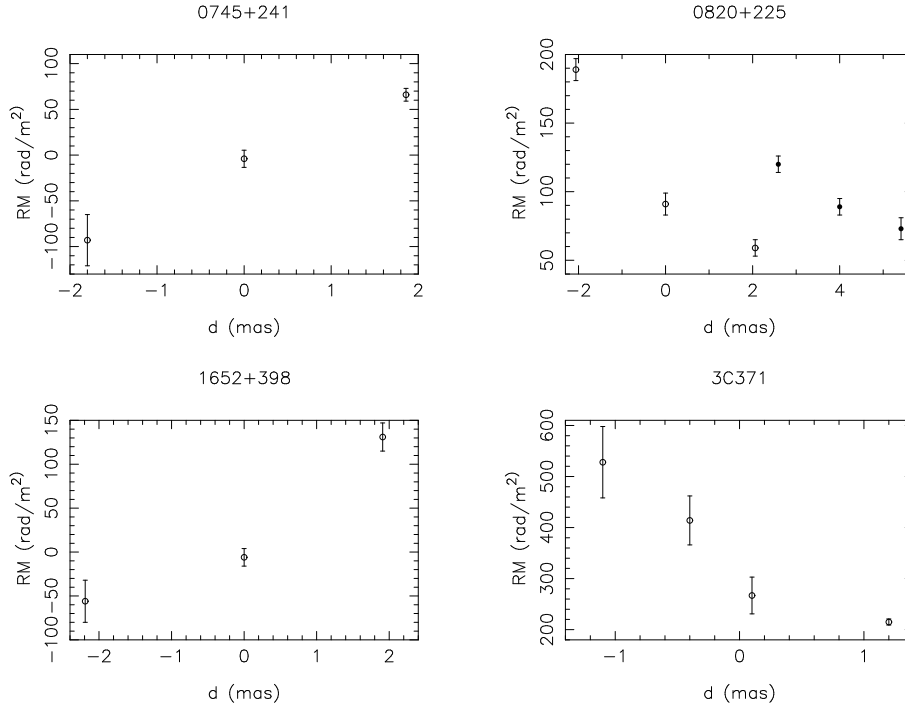


Figure 2. Plots of observed rotation measure as a function of transverse distance d from a reference point P near the central jet spine for cuts along the indicated position angles PA across the jets of the four objects shown in Fig. 1. Top left (0745+241): $P = (-1.5 \text{ mas}, 0.7 \text{ mas})$, d measured along $PA = 35^\circ$, with northeast d being negative. Top right (0820+225): open circles show the results for $P = (-8.6 \text{ mas}, -6.7 \text{ mas})$, d measured along $PA = -60^\circ$, with southeast d being negative; filled circles shown the results for $P = (-11.6 \text{ mas}, -9.6 \text{ mas})$, d measured along $PA = -45^\circ$, with southeast d being negative. The distances for the latter three RM values have been arbitrarily shifted 4.0 mas to ease viewing of the results for both cuts in a single plot. Bottom left (1652+398): $P = (3.0 \text{ mas}, -3.2 \text{ mas})$, d measured along $PA = 50^\circ$, with northeast d being negative. Bottom right (3C371): $P = (5.4 \text{ mas}, -0.5 \text{ mas})$, d measured along $PA = 0^\circ$, with south d being negative. All errors are 2σ .

tion having a common origin, but it is obviously impossible to know if this is a coincidence on the basis of only these two sources. It will be of considerable interest to carry out joint analyses of the RM gradients and core circular polarizations for additional sources as more data become available to see if these two quantities are, indeed, related.

5 CONCLUSION

Our analysis has demonstrated the presence of Faraday-rotation gradients transverse to the VLBI jets of four BL Lac objects. These transverse RM gradients provide compelling new evidence that the jet **B** fields of these objects are dominated by the toroidal component, indicating that the **B** fields themselves are either toroidal or helical. This represents the first direct observational evidence for toroidal or helical **B**-field structures associated with the jets of AGN.

This has fundamental implications for our understanding of the launching and propagation of these jets; in particular, it is clear that we must think of the jets as fundamentally electromagnetic structures. These results provide support for models in which the launching of the jets is associated with a seed **B** field initially threading the accretion disk that is wound up by the rotation of the disk and central black hole. This has seemed like an obvious possibility from the theoretical point of view, but until now, there has been no observational evidence that directly supported such mod-

els. In addition, the presence of helical fields would provide a natural mechanism for collimating the jets.

An analysis of the parsec-scale RM distributions for remaining sources in the Kühr & Schmidt (1990) sample of BL Lac objects is underway, and results will be presented in a future paper, where we will also consider the question of to what extent transverse RM gradients are characteristic of the sample as a whole. We are also in the process of obtaining new multi-wavelength VLBA polarization observations for all the sources in this sample of BL Lac objects, designed to be better optimized for Faraday-rotation studies; these new observations should enable us to both confirm the results obtained thus far and to study the parsec-scale RM distributions with appreciably better resolution.

6 ACKNOWLEDGEMENTS

We thank the referee for useful and pertinent comments, as well as for prompt reviewing of the manuscript. The National Radio Astronomy Observatory is operated by Associated Universities, Inc., under cooperative agreement with the NSF.

REFERENCES

Asada K. et al. 2002, PASJ, 54, L39

- Blandford R. D. 1993, in *Astrophysical Jets* (Cambridge University Press), p. 26
- Blandford R. D. & Königl A. 1979, *ApJ*, 232, 34
- Burn B. J. 1966, *MNRAS*, 133, 67
- Croke S., Charlot P., Gabuzda D. C. & Sol H. 2004, in *Radio Astronomy at 70: from Karl Jansky to Microjansky*, Baltic Astronomy, in press
- Gabuzda D. C. 1999, *New Astron. Rev.*, 43, 691
- Gabuzda D. C. 2003, *New Astron. Rev.*, 47, 599
- Gabuzda D. C. & Cawthorne T. V. 1996, *MNRAS*, 283, 759
- Gabuzda D. C. & Chernetskii V. A. 2003, *MNRAS*, 339, 669
- Gabuzda D. C. & Gómez J. L. 2001, *MNRAS*, 320, L49
- Gabuzda D. C., Mullan C. M., Cawthorne T. V., Wardle J. F. C., & Roberts D. H. 1994, *ApJ*, 435, 140
- Gabuzda D. C. & Pushkarev A. B. 2002, in “Particles and Fields in Radio Galaxies,” R. Laing and K. Blundell, Eds. (Astronomical Society of the Pacific, San Francisco, 2002), ASP Conf. Ser. 250, p. 180
- Gabuzda D. C., Pushkarev A. B. & Cawthorne T. V. 2000, *MNRAS*, 319, 1109
- Gabuzda D. C., Pushkarev A. B., & Garnich 2001, 327, 1
- Gabuzda D. C. & Vitrichchak M. V. 2004, in *Radio Astronomy at 70: from Karl Jansky to Microjansky*, Baltic Astronomy, in press
- Homan D. C., Attridge J. M. & Wardle J. F. C. 2001, *ApJ*, 556, 113
- Hughes P. A., Aller H. D. & Aller M. A. 1989, *ApJ*, 341, 68
- Hujeirat A., Livio M., Camenzind M. & Burkert A. 2003, *A&A*, 408, 415
- Kühr H. & Schmidt G. D. 1990, *AJ*, 90, 1
- Laing R. 1980, *MNRAS*, 193, 439
- Lovelace R. V. E., Li H., Koldoba A. V., Ustyugova G. V. & Romanova M. M. 2002, *ApJ*, 572, 445
- Lynden-Bell D. 2003, *MNRAS*, 341, 1360
- Lyutikov M. 2003, *New Astron. Rev.*, 47, 513
- Nakamura M., Uchida Y., Hirose S. 2001, *New Astron.*, 6, 61
- Pariev V. I., Istomin Ya. N. & Beresnyak A. R. 2003, *A&A*, 403, 805
- Pushkarev A. B. 2001, *Astron. Rep.*, 45(9), 667
- Reynolds C., Cawthorne T. V., & Gabuzda D. C. 2001, *MNRAS*, 327, 1071
- Tsinganos K. & Bogovalov S. 2002, *MNRAS*, 337, 553
- Wardle J. F. C., Roberts D. H. & Brown L. F. 1994, *ApJ*, 427, 718
- Zavala R. T. & Taylor G. B. 2003, *ApJ*, 589, 126